HHS Public Access

Author manuscript

Arthritis Rheumatol. Author manuscript; available in PMC 2021 February 01.

Published in final edited form as:

Arthritis Rheumatol. 2020 February ; 72(2): 335–347. doi:10.1002/art.41076.

Genetic deficiency of IFNγ reveals IFNγ-independent manifestations of murine Hemophagocytic Lymphohistiocytosis

Thomas N Burn, BSc[1,2], **Lehn Weaver, MD, PhD**[2], **Julia E Rood, MD, PhD**[1,2], **Niansheng Chu, MD**[2], **Aaron Bodansky, MD**[2], **Portia A Kreiger, MD**[3], **Edward M Behrens, MD**[1,2]

[1]Institute for Immunology, Perelman School of Medicine, University of Pennsylvania, Philadelphia, PA

[2]Division of Rheumatology, The Children's Hospital of Philadelphia, Philadelphia, PA

[3]Department of Pathology, The Children's Hospital of Philadelphia, Philadelphia, PA

Abstract

Objective: Familial hemophagocytic lymphohistiocytosis (FHL) is a complex cytokine storm syndrome caused by genetic abnormalities rendering CD8+ T cells and NK cells incapable of cytolytic killing. Murine models of FHL have identified interferon-gamma (IFNγ) made by CD8+ T cells as a critical mediator of disease, with an IFNγ-blocking antibody (Emapalumab) recently receiving FDA approval. However, development of hemophagocytic lymphohistiocytosis (HLH)/ macrophage activation syndrome (MAS) in patients who are genetically unresponsive to IFNγ questions the absolute necessity of IFNγ in driving disease. The purpose of this study was to determine the necessity for IFNγ in driving HLH.

Methods: *IFNγ*$^{-/-}$*Prf1*$^{-/-}$ mice were infected with LCMV and HLH immunopathologic features, including survival, weight-loss, cytopenias, cytokine profiles, and immune cell phenotypes were assessed. Mixed bone marrow chimeras were created to determine the immune-cell intrinsic role of IFNγR-signaling. CD8+ T cell depletion and IL-33:ST2 blockade was performed using monoclonal antibodies.

Results: LCMV infection of *IFNγ*$^{-/-}$*Prf1*$^{-/-}$ mice results in severe HLH-like disease. CD8+ T cells, and the IL-33:ST2 axis remain essential mediators of disease, however, IFNγ-independent HLH immunopathology correlates with 10–15 fold increased neutrophilia ($p<0.001$) and an altered cytokine milieu dominated by IL-6, IL-1β, and GM-CSF ($p<0.05$). Furthermore, IFNγ regulates CD8+ T cell expression of GM-CSF, and neutrophil survival.

Conclusion: IFNγ is not necessary for development of fulminant HLH requiring physicians to consider case-by-case treatment strategies. Use of therapies that target upstream activators of

Corresponding Author: Edward M Behrens, MD, 3615 Civic Center Boulevard, 1102 Abramson Research Center, Philadelphia, PA 19104-4399, USA, Tel: 1-267-426-0142; behrens@email.chop.edu.

AUTHOR CONTRIBUTIONS

TNB designed and performed the experiments and wrote the manuscript. LW and JER helped with experiments and manuscript editing. NC and AB helped with experiments. PK took the histology photographs and provided pathologic interpretation. EMB designed experiments and wrote the manuscript.

Conflict of Interests: J.E.R. and E.M.B. are named on U.S. Patent #:10,040,859 "Methods of treating hemophagocytic lymphohistiocytosis with an IL-33 receptor antibody". The authors have no additional financial interests.

CD8+ T cells, such as IL-33:ST2 signaling, may be more universally applicable treatment options that ameliorate both IFNγ-dependent and -independent manifestations of HLH/MAS.

INTRODUCTION

Hemophagocytic lymphohistiocytosis (HLH) is life-threatening cytokine storm syndrome, characterized by over-abundance and over-activation of CD8+ T cells(1). The genetic abnormalities that underlie familial forms of HLH (FHL) have been traced to genes involved in the cytolytic capabilities of cytotoxic lymphocytes(2). Currently, the only effective cure for FHL is bone marrow transplantation. The best characterized and most frequently identified genetic lesions occur in the perforin gene (*Prf1*) and define FHL2 patients. The inability to clear antigen through perforin-dependent cytolysis by CD8+ T cells leads to protracted antigen exposure, increased CD8+ T cell proliferation, activation, and exaggerated inflammatory cytokine production, thought to drive immunopathology(3, 4).

Studies utilizing the perforin knockout mouse ($Prf1^{-/-}$) have implicated the excessive production of interferon gamma (IFNγ) by hyper-active CD8+ T cells as the primary driver of disease(3). Antibody-mediated depletion of CD8+ T cells, and antibody-mediated blockade of IFNγ are effective in preventing disease in multiple murine models of FHL(3, 5). Additionally, we have recently identified IL-33 signaling through ST2 as an additional upstream activator of CD8+ T cells that is essential in driving CD8+ T cell hyperactivation(6, 7). These data have spurred a clinical trial investigating antibody-mediated blockade of IFNγ (Emapalumab) in human HLH patients that has recently resulted in FDA approval(8).

HLH diagnoses in the absence of obvious genetic lesions in known FHL genes are defined by a set of clinical criteria, leaving scope for many causative triggers and pathological effectors(9). Despite the precedence that HLH disease pathogenesis is dependent on IFNγ, several murine models have shown that HLH-disease can be driven by alternative cytokines(10, 11). Additionally, a number of patients have developed HLH-like or Macrophage Activation Syndrome (MAS)-like disease in the setting of mutations in the IFNγ receptor rendering them unresponsive to IFNγ(12–14). This suggests that HLH/MAS physiology can result independent of IFNγ, or that IFNγ can signal through an alternative receptor to drive disease in these settings. Other preclinical models of murine HLH in mice that lack IFNγ or a functional IFNγ receptor (IFNγR), have not been adequately incorporated into most explanations of disease pathogenesis(15, 16).

To query the absolute necessity of IFNγ in driving HLH, we infected $IFN\gamma^{-/-}Prf1^{-/-}$ double knockout mice with LCMV. Herein, we demonstrate that LCMV infection is sufficient to drive HLH-like pathology in the absence of IFNγ. LCMV-infected $IFN\gamma^{-/-}Prf1^{-/-}$ double knockout mice have disease of equal lethality to $Prf1^{-/-}$ mice. A modified qualitative response is highlighted by an altered serum cytokine signature and extensive neutrophilia, reminiscent of that which is seen in Systemic Juvenile Idiopathic Arthritis (sJIA) associated MAS(17). Despite loss of IFNγ production, CD8+ T cells and ST2 signaling remain essential in the pathogenesis of IFNγ-independent HLH-like disease. Additionally, in the absence of IFNγ signaling, CD8+ T cells have heightened GM-CSF producing capacity,

unveiling an unrecognized method of GM-CSF regulation. These results highlight important regulatory roles for IFNγ in inflammatory conditions, which may be informative for diseases in which neutrophilia and/or aberrant GM-CSF production are pathogenic. Furthermore, this study addresses a clinically relevant and under-appreciated aspect of HLH biology by defining IFNγ-independent cytokine storm pathology.

MATERIALS AND METHODS

Mice

C57BL/6(WT), perforin deficient(C57BL/6-Prf1^{tm1Sdz}/J, *Prf1*$^{-/-}$), interferon-gamma deficient(B6.129S7-Ifng^{tm1Ts}/J, *IFNγ*$^{-/-}$), interferon gamma receptor deficient(B6.129S7-Ifngr1^{tm1Agt}/J, *IFNγR*$^{-/-}$), and B6-CD45.1(B6.SJL-Ptprc^{a} Ptprc^{b}/BoyJ) mice were purchased from The Jackson Laboratory and bred in our facility. Prf1$^{-/-}$ mice were crossed to *IFNγ*$^{-/-}$ mice, *IFNγR*$^{-/-}$ mice, and B6-CD45.1 mice. All animal studies performed with approval from The Children's Hospital of Philadelphia Institutional Animal Care and Use Committee

Induction of FHL

6 to 8-week old mice were infected intraperitoneally with 2×10^5 plaque-forming units of LCMV-Armstrong and euthanized upon development of significant morbidity or weight loss. Peripheral blood cell counts were performed by the Translational Core Laboratory on the Sysmex XT-2000iV Automated Hematology Analyzer at The Children's Hospital of Philadelphia. Serum ferritin (ALPCO), soluble CD25 (R&D Systems), IL-6, GMCSF, IL-1β, and IFNγ (BD Biosciences) were measured by ELISA. Plaque assay was performed on Vero cells as previously described(18).

Histology

All slides were stained with hematoxylin and eosin. Images were acquired on an Eclipse 90i microscope (Nikon, Melville, NY) using NIS-ELEMENTS software.

Analysis of human gene expression

Published data set (GSE26050)(19) was accessed through the National Center for Biotechnology Information Gene Expression Omnibus. IFNγ-gene-set (HALLMARK_INTERFERON_GAMMA_RESPONSE) was downloaded from the MSigDB (Broad Institute). Hierarchical clustering and heatmaps were performed using Morpheus (Broad Institute).

Flow cytometric analysis

Peripheral blood leukocytes, splenocytes, intrahepatic leukocytes, and bone marrow leukocytes were stained with LIVE/DEAD fixable viability dye (Life Technologies), anti-CD90.2, CD19, NK1.1, CD11b, Ly6G, Ly6C, CD4, CD8α, CD44, CD62L, CD45.2, and CD45.1 (BD Pharmingen, eBioscience, and Biolegend). H-2D^{b}GP$_{33–41}$ MHC-peptide complexes were provided as fluorophore-conjugated tetramers by Dr. E.J. Wherry

(University of Pennsylvania). Samples were acquired on a MACSQuant flow cytometer (Miltenyi Biotec) and analyzed using Flowjo software version 10.4.2.

Intracellular cytokine staining

Splenocytes (10^6) were stimulated with 50ng/ml PMA (Sigma), 1μg/ml ionomycin (Cell Signaling Technology), 2μg/ml brefeldin A (Sigma) and 2μM monensin (eBioscience) for 5 hours at 37°C. After staining for LIVE/DEAD and surface antigens as before, cells were stained for IFNγ (clone XMG1.2 - BD) and GM-CSF (clone MP1–22E9 - BD) using the Cytofix/Cytoperm kit (BD Bioscience).

In vivo antibody and recombinant IFNγ administration

Antibodies were delivered intraperitoneally beginning day 3 post-infection and every other day thereafter. Dosing and antibodies used as following: CD8 depletion, 500μg (clone 2.43, BioXcell), IgG2b isotype control (clone LTF-2, BioXcell). ST2 blockade as previously described using antibody provided by Amgen (20, 21). Cytokine blockade; 500μg anti-IFNγ (clone XMG1.2, BioXcell), 200μg anti-IL6R (clone15A7, BioXcell), 200μg anti-IL-1β (clone B122, BioXcell), 100μg anti-GM-CSF (clone MP1–22E9, BioXcell), and same dose of respective isotype controls (BioXcell). For recombinant-IFNγ give-back experiments, mice were administered 10μg recombinant-IFNγ (Peprotech) every other day beginning either day 0, or day 6 post-infection.

In vitro CD8+ T cell GM-CSF production assay

Naïve (CD44-) CD8+ T cells were enriched from naïve *IFNγ*$^{-/-}$ mice using Naïve CD8a+ T cell isolation kits (Miltenyi). Purity was consistently greater than 90%. Cells were cultured on plate-bound anti-CD3 (2μg/ml - Biolegend) and anti-CD28 (2μg/ml - Biolegend) in 96 well flat-bottomed plates with 10ng/ml recombinant murine IL-12 (Peprotech) and 50U/ml human IL-2 (Peprotech) for 2 days. Cells were removed from anti-CD3/28, cultured a further 2 days with IL-2 and IL-12, before 1 day with IL-2 alone. CD8s were re-stimulated with PMA and ionomycin and stained for intracellular GM-CSF as before.

Generation of bone marrow chimeras

6 to 8-week-old host (*Prf1*$^{-/-}$*IFNγR*$^{+/+}$*CD45.1*$^{+/+}$) mice were lethally irradiated (950Rad - X-RAD irradiator). Bone marrow was isolated from donor strains (*Prf1*$^{-/-}$*IFNγR*$^{+/+}$*CD45.1*$^{+/+}$ and *Prf1*$^{-/-}$*IFNγR*$^{-/-}$*CD45.2*$^{+/+}$), mixed 1:1, and 5×10^6 bone marrow cells were injected intravenously to host mice 6-hours post-irradiation. Chimeras were reconstituted for 8 weeks before LCMV-infection.

Apoptosis assay

Bone marrow from day 10 post-infection chimeric mice was incubated at 37°C. Cells were stained for active caspase3/7 using the Vybrant® FAM Caspase-3/7 assay kit (ThermoFisher) as per the manufacturer's directions. Cells were then stained with LIVE/DEAD and surface antigens as before.

Statistical analyses

Weight loss data was analyzed by linear mixed-effects models using R (R Core Team, 2014), and *lme4*. Visual inspection of residual plots did not reveal any obvious deviations from homoscedasticity or normality. P values were obtained by likelihood ratio tests of the full model with the effect in question against the model without the effect in question. All other data were analyzed in Graphpad Prism 7 using statistical tests indicated in the figure legends.

RESULTS

IFNγ$^{-/-}$Prf1$^{-/-}$ mice succumb to HLH-like disease

To determine whether IFNγ was necessary for fulminant HLH development in the murine FHL2 model, we generated *IFNγ*$^{-/-}$*Prf1*$^{-/-}$ double knockout mice and observed HLH clinical characteristics following LCMV infection. *IFNγ*$^{-/-}$*Prf1*$^{-/-}$ and *Prf1*$^{-/-}$ mice experience equivalent mortality, (Figure 1A) and significant weight loss, despite this not being quite as severe (Figure 1B). WT and *IFNγ*$^{-/-}$ mice clear LCMV-Arm(22), display no mortality or weight loss, and are used as controls throughout. While *IFNγ*$^{-/-}$*Prf1*$^{-/-}$ mice do not experience anemia (Figure 1C), suggesting an IFNγ-dependent effect, both *IFNγ*$^{-/-}$*Prf1*$^{-/-}$ and *Prf1*$^{-/-}$ mice have severe thrombocytopenia (Figure 1D). Interestingly, while leukopenia is a common feature in HLH pathology, *IFNγ*$^{-/-}$*Prf1*$^{-/-}$ mice have elevated leukocyte counts (Figure 1E). *IFNγ*$^{-/-}$*Prf1*$^{-/-}$ mice have extremely elevated sCD25 levels (Figure 1F) suggesting the presence of highly activated T cells, have serum ferritin levels equivalent to *Prf1*$^{-/-}$ mice (Figure 1G), and hepatosplenomegaly equivalent to *Prf1*$^{-/-}$ mice (Figure 1H, I). Finally, hemophagocytes were readily identified in spleens of *IFNγ*$^{-/-}$*Prf1*$^{-/-}$ mice (Figure 1J). Given NK cell function is defective by virtue of perforin absence, *IFNγ*$^{-/-}$*Prf1*$^{-/-}$ mice fulfill 5 criteria required for HLH diagnosis and partially fulfill a sixth in terms of cytopenia(9). Importantly, splenic viral titers between *Prf1*$^{-/-}$ and *IFNγ*$^{-/-}$*Prf1*$^{-/-}$ are not different at day 10 post-infection (Supplemental Figure 1).

Unlike genetic deficiency, antibody-mediated blockade of IFNγ protects *Prf1*$^{-/-}$ mice from most disease features. We suspected that such blockade is not 100% efficient, explaining this difference. We therefore compared expression of the IFNγ-induced gene MHCII on inflammatory monocytes in Prf1$^{-/-}$ mice treated with anti-IFNγ blocking antibody, and IFNγ$^{-/-}$Prf1$^{-/-}$ mice. Incomplete IFNγ blockade by antibody is suggested based on incomplete reduction in MHCII expression (Supplemental Figure 2). Taken together, these data indicate that many clinical features of HLH pathology can arise independent of IFNγ, and that low level IFNγ signaling correlated with protection from disease.

IFNγ$^{-/-}$Prf1$^{-/-}$ mice display extensive neutrophilia

Leukocyte counts were extremely high in *IFNγ*$^{-/-}$*Prf1*$^{-/-}$ mice compared to *Prf1*$^{-/-}$ and WT/*IFNγ*$^{-/-}$ controls and were predominantly neutrophils (Figure 2A). Increased neutrophils were also seen in spleens and livers of *IFNγ*$^{-/-}$*Prf1*$^{-/-}$ mice following LCMV infection (Figure 2B–C, Supplemental Figure 3). Histological analysis of livers from *IFNγ*$^{-/-}$*Prf1*$^{-/-}$ mice reveals the presence of mature neutrophils as determined by observation of ringed/multi-lobed nuclei (Figure 2D – arrows). Neutrophils were not observed in any

significant quantity in *Prf1*$^{-/-}$ livers. Additionally, liver histology shows that while *Prf1*$^{-/-}$ mice have extensive hepatosteatosis (Figure 2D), this is absent in *IFNγ*$^{-/-}$*Prf1*$^{-/-}$ mice, suggesting an IFNγ-dependent phenomenon. *IFNγ*$^{-/-}$*Prf1*$^{-/-}$ mice also have large amounts of peri-portal inflammation, surpassing that of *Prf1*$^{-/-}$ mice. Together, extensive neutrophilia is a predominant feature of HLH in the absence of IFNγ.

Altered cytokine milieu in *IFNγ*$^{-/-}$*Prf1*$^{-/-}$ mice corresponds with cytokine expression in human HLH patients

Serum IL-6, granulocyte-macrophage colony stimulating factor (GM-CSF), and IL-1β were all significantly elevated in *IFNγ*$^{-/-}$*Prf1*$^{-/-}$ mice compared to *Prf1*$^{-/-}$ and control mice (Figure 3A–C), while *Prf1*$^{-/-}$ mice had extremely high levels of serum IFNγ (Figure 3D). Individual blockade of IL-6, IL-1β, or GM-CSF did not provide major protection from disease in *IFNγ*$^{-/-}$*Prf1*$^{-/-}$ mice (supplemental figure 4) despite dosing of blocking antibodies that was equivalent to that used in other settings(23–25).

We next made use of a publicly available dataset that profiled gene expression from PBMCs of patients with active HLH to compare their cytokine profiles to this mouse model (19). This dataset included both HLH patients with identified perforin mutations or no identified genetic cause (Figure 3E-green bar) and healthy controls (Figure 3E-grey bar). While it was previously described that this dataset did not find a statistically significant difference in expression of IFNγ-induced transcripts between HLH patients and controls, we were curious to examine whether such an IFNγ-signature could be used to discriminate between patients and controls, and the extent to which patients might have differing IFNγ-signatures. To do this we filtered on IFNγ-stimulated genes (MSigDB-Broad Institute) and performed unsupervised hierarchical clustering (Figure 3E). It is clear that HLH-patients cluster separately from controls, something not interpretable in gene-set enrichment analyses. Secondly, the HLH patients separate into two major groups; cluster-i having a high IFNγ-signature, and the cluster-ii having a lower IFNγ-signature. Cluster-i is a clear and closely related cluster, while cluster-ii is more diverse and probably best described as ‘other’. These two major clusters are defined by three main groups of genes. Group-a shows high expression in both patient clusters and includes *IL6, TNFAIP6, TNFAIP3, SOCS3, STAT3*, which are upregulated by a number of cytokines including IL-6 and TNF. Group-b shows elevated expression in patient cluster-i, depression in cluster-ii, and includes the genes *STAT1, CXCL10, IFIT3*, and MX1, which are classical IFNγ response genes. Finally, group-c indicates genes depressed in both patient clusters. Group-c includes *BANK1*, suggesting selective absence of B cells from the PBMCs of all patients, and *CIITA* indicating downregulation of MHCII or absence of B-cells or APCs. Overall this agrees with the previous report suggesting the absence of a strong IFNγ-signature among HLH-patients(19), yet this analysis makes it clear that the gene expression changes are more complicated than a wholesale absence of an IFNγ-response. It may rather highlight that some patients may have very strong IFNγ-signatures, and others may have weaker signatures. It is important to note that perforin-deficient patients did not cluster separately from patients with no identified mutation.

We were then interested to examine the expression of other cytokines that were expressed. Patients falling within the high IFNγ-signature cluster tended to have higher expression of other cytokines (Figure 3E-bottom), but expression of key cytokines such as *IL-1β, TNF, and IL6* remained elevated in all patients over controls despite partially divergent IFNγ-signatures among patients. Thus, there exist a set of patients with weak IFNγ-signature, but overexpression of non-IFNγ cytokines, consistent with the idea of non-IFNγ HLH.

CD8+ T cells from *IFNγ*$^{-/-}$*Prf1*$^{-/-}$ mice have elevated expression of GM-CSF that is regulated by exogenous IFNγ

CD8+ T cells are appreciated to be central mediators of pathology in other murine models of HLH, including the *Prf1*$^{-/-}$ model(3). We asked whether CD8+ T cells were expanded in LCMV-infected *IFNγ*$^{-/-}$*Prf1*$^{-/-}$ mice utilizing H-2D^{b}-gp33 tetramers to examine the expansion of LCMV-specific CD8+ T cells. Virus-specific *IFNγ*$^{-/-}$*Prf1*$^{-/-}$ CD8+ T cells expand to equivalent frequencies and total numbers in the spleen compared to *Prf1*$^{-/-}$ mice (Figure 4A, B).

Because of the elevated serum GM-CSF observed in the *IFNγ*$^{-/-}$*Prf1*$^{-/-}$ mice, the expansion of *IFNγ*$^{-/-}$*Prf1*$^{-/-}$ CD8+ T cells, and that CD8+ T cells are known to make GM-CSF in other settings(26, 27), we asked whether CD8+ T cells made GM-CSF in LCMV-infected *IFNγ*$^{-/-}$*Prf1*$^{-/-}$ mice. We observed that GM-CSF-producing CD8s were elevated in both frequency and number in LCMV-infected *IFNγ*$^{-/-}$*Prf1*$^{-/-}$ mice compared to WT, *Prf1*$^{-/-}$, and *IFNγ*$^{-/-}$ mice (Figure 4C, D, Supplemental Figure 5). Similar trends were seen for CD4+ T cells, however CD8+ T cells in LCMV-infected *IFNγ*$^{-/-}$*Prf1*$^{-/-}$ mice outnumbered CD4+ T cells by 10-fold (data not shown).

Given these findings, we hypothesized that IFNγ negatively regulates the expression of GM-CSF by CD8+ T cells. We therefore infected *IFNγ*$^{-/-}$*Prf1*$^{-/-}$ mice with LCMV and provided exogenous, recombinant IFNγ to these mice every other day from either day 6 post infection (rIFNγ short) or for the entirety of the 10-day experiment (rIFNγ long) and compared the expression of GM-CSF in CD8+ T cells from these mice to littermate LCMV-infected *IFNγ*$^{+/-}$*Prf1*$^{-/-}$ controls. The addition of rIFNγ was sufficient to restore systemic IFNγ signaling, as the IFNγ-stimulated gene, MHCII, was induced on inflammatory monocytes in *IFNγ*$^{-/-}$*Prf1*$^{-/-}$ mice treated with rIFNγ (Supplemental Figure 6). Consistent with our hypothesis, rIFNγ inhibited the expression of GM-CSF by CD8+ T cells in a dose-dependent manner (Figure 4E, F). Additionally, we cultured naïve *IFNγ*$^{-/-}$ CD8+ T cells *in vitro* for 5-days with or without the addition of exogenous IFNγ and show that CD8+ T cells exposed to IFNγ have decreased GM-CSF expression (Figure 4G, H). These data support the notion that IFNγ negatively regulates the expression of GM-CSF by CD8+ T cells.

Neutrophil-intrinsic IFNγ-signaling regulates neutrophilia through enhanced cell death

In many HLH patients where IFNγ is thought to drive disease, neutropenia correlates with disease severity(28), contrasting with the extensive neutrophilia observed in *IFNγ*$^{-/-}$*Prf1*$^{-/-}$ mice. This led us to question whether IFNγ has a direct effect on neutrophilia. First, we asked if restoration of recombinant IFNγ to *IFNγ*$^{-/-}$*Prf1*$^{-/-}$ mice would blunt neutrophilia during LCMV infection. *IFNγ*$^{-/-}$*Prf1*$^{-/-}$ mice were infected with LCMV and recombinant

IFNγ was given every other day for the full 10-day infection (rIFNγ-long) or from day 6 post infection (rIFNγ-short), and blood neutrophil counts were compared to controls. Blood neutrophil counts were decreased in a dose-dependent manner when IFNγ was restored suggesting that IFNγ suppresses neutrophilia in LCMV-infected *IFNγ*$^{-/-}$*Prf1*$^{-/-}$ mice (Figure 5A).

To determine whether this effect was a neutrophil-intrinsic phenomenon we made *IFNγR*$^{-/-}$*Prf1*$^{-/-}$:*IFNγR*$^{+/+}$*Prf1*$^{-/-}$ mixed bone-marrow chimeras and subsequently infected them with LCMV. The ratio of *IFNγR*$^{-/-}$*Prf1*$^{-/-}$ to *IFNγR*$^{+/+}$*Prf1*$^{-/-}$ leukocyte populations was determined, and we could show IFNγ-unresponsive T cells, neutrophils, and inflammatory monocytes, outcompeted IFNγ-responsive cells (Figure 5B–D, Supplemental Figure 7). *IFNγR*$^{-/-}$*Prf1*$^{-/-}$ B cells outcompeted IFNγ-responsive cells in the spleen and blood, but interestingly not in the bone-marrow. The most profound effects occurred on the myeloid-derived cell populations suggesting that the IFNγ-mediated suppression of neutrophilia occurs in a myeloid cell-intrinsic manner. Accordingly, common-myeloid-progenitors(CMPs), granulocyte-monocyte-progenitors(GMPs), and monocyte-dendritic cell-progenitors(MDPs) all were selectively enriched in the IFNγR$^{-/-}$ genotype (Supplemental Figure 8A–B). Staining of the proliferation marker Ki67 indicated no difference in proliferation of myeloid-precursors between donor genotypes (Supplemental Figure 8C).

Neutrophils are typically a short-lived cell type, with a lifespan in mice of approximately 12.5 hours(29). Therefore, alterations in the lifespan of neutrophils can have profound downstream effects on their accumulation. We sought to determine whether neutrophil-intrinsic IFNγ-signaling impacted the survival of neutrophils. Bone marrow from day 10 infected *IFNγR*$^{-/-}$*Prf1*$^{-/-}$:*IFNγR*$^{+/+}$*Prf1*$^{-/-}$ mixed bone-marrow chimeras was assayed for active caspase3/7 and plasma membrane permeability directly *ex vivo* (T=0hrs), or after 6 or 24-hours in vitro. Neutrophils unable to respond to IFNγ displayed striking protection from apoptosis (Figure 5E, F) suggesting IFNγ limits the lifespan and therefore total accumulation of mature neutrophils in a cell-intrinsic manner.

CD8+ T cells and IL-33-signaling remain pathological drivers of disease in the absence of IFNγ

Hyperactivation of CD8+ T cells is closely linked to HLH immunopathology in IFNγ sufficient murine models of disease(3, 21). To determine whether CD8+ T cells are necessary for disease in the absence of IFNγ, *IFNγ*$^{-/-}$*Prf1*$^{-/-}$ mice were infected with LCMV before CD8 depletion was initiated beginning day 3 post-infection. *IFNγ*$^{-/-}$*Prf1*$^{-/-}$ mice depleted of CD8+ T cells were protected from death (Figure 6A), and weight-loss (Figure 6B) compared to isotype-treated controls. CD8+ T cell depletion also resulted in protection from neutrophilia (Figure 6C) suggesting that *IFNγ*$^{-/-}$*Prf1*$^{-/-}$ CD8+ T cells provide a signal that enhances neutrophil differentiation, survival, and/or persistence in the bloodstream.

Given our previous work showing that the IL-33:ST2 axis was a crucial upstream mediator of CD8+ T cell effector function leading to their pathological role in LCMV-infected *Prf1*$^{-/-}$ mice(7, 21), we sought to determine whether IL-33 is required for HLH in the absence of

IFNγ. *IFNγ*$^{-/-}$*Prf1*$^{-/-}$ mice were infected with LCMV, and ST2 was blocked beginning day 3 post-infection. ST2 blockade remained effective in *IFNγ*$^{-/-}$*Prf1*$^{-/-}$ mice providing significant protection from weight loss (Figure 6D), by χ^2-analysis of total survival at day 10 post-infection (7/12 isotype controls vs. 11/11 anti-ST2 blocked mice alive, p=0.037, Fisher's exact test), as well as reducing serum sCD25 (Figure 6E) and serum ferritin (Figure 6F). The frequency of effector phenotype CD8+ T cells correlated with the total weight loss observed in ST2 blocked and isotype blocked mice suggesting a link between decreased CD8+ T-cell activation and disease activity (Figure 6G, Supplemental Figure 9). Given the role of CD8+ T cells in driving disease in *IFNγ*$^{-/-}$*Prf1*$^{-/-}$ mice, we speculate that IL-33:ST2 signaling drives effector differentiation of *IFNγ*$^{-/-}$*Prf1*$^{-/-}$ CD8+ T cells and that this differentiation is essential for driving disease. In addition, ST2 blockade completely ameliorated neutrophilia in *IFNγ*$^{-/-}$*Prf1*$^{-/-}$ mice (Figure 6H). We hypothesize that this is due to reduced CD8+ T cell activation which we know is needed for the neutrophilia, yet it is also known that IL-33 signaling can act directly on neutrophils to exacerbate inflammation(30). Overall, these data show that IFNγ is not necessary for development of a CD8-driven HLH-like disease in a novel murine model.

DISCUSSION

While much effort has been exerted into targeting the effects of IFNγ signaling in treating HLH/FHL, a growing body of literature suggests that HLH is a diverse disease triggered by various agents, under many genetic and pathological conditions, with a range of mortality-inducing end stage effectors. We now provide additional support to this notion by showing that HLH-like pathogenesis can occur in the genetic absence of IFNγ. Investigating doubly deficient *IFNγ*$^{-/-}$*Prf1*$^{-/-}$ mice shows that IFNγ is not absolutely necessary for disease, identifies IFNγ-dependent facets of HLH, and makes important observations of the regulatory roles of IFNγ in regulation of neutrophil survival and CD8+ T-cell responses to viral infection.

We show that HLH can develop in the genetic absence of IFNγ. Consistent with our data, LCMV-Traub infection of *IFNγ*$^{-/-}$*Prf1*$^{-/-}$ mice on a mixed B6/129SV background(16), and murine gammaherpesvirus 68 (MHV68) infection of *IFNγ*$^{-/-}$*Prf1*$^{-/-}$ mice caused significant mortality(31). In a model of secondary HLH, BALB/c mice infected with cytomegalovirus succumbed to HLH-like disease, and genetic absence of IFNγ enhanced disease severity(32). The same group has described in multiple reports the suppressive role for IFNγ in a murine model of sJIA, a disease well known to be prone to MAS(17, 33). Additionally, a recent report investigating mechanisms of HLH in *IFNγR*$^{-/-}$*Prf1*$^{-/-}$ mice agree with our findings and show development of HLH-like disease, in the absence of IFNγ-signaling. Interestingly this report details the role of CD25 signaling in the propagation of disease, and similarly *IFNγR*$^{-/-}$*Prf1*$^{-/-}$ mice have higher serum sCD25 than *Prf1*$^{-/-}$ mice(34). This difference in sCD25 may be a result of the increased activation state of the CD8s in the absence of IFNγ (data not shown)(34). Thus, our data contributes to a growing body of literature that IFNγ is not absolutely required for HLH disease manifestation. Our report is the first complete description of primary HLH disease in the genetic absence of IFNγ and advances the clinical description of IFNγ-independent HLH pathology. Importantly, diagnostic and clinical features of HLH such as hepatosplenomegaly, thrombocytopenia,

elevated serum ferritin, elevated soluble CD25, hemophagocytosis, and hepatitis remain present despite the absence of IFNγ, highlighting the need to expand the model of pathogenesis beyond this cytokine.

While *Prf1*$^{-/-}$ and *IFNγ*$^{-/-}$*Prf1*$^{-/-}$ mice do not present with identical disease, the most important indicators of mortality and morbidity are not different. Of note, anemia is not a significant problem in the *IFNγ*$^{-/-}$*Prf1*$^{-/-}$ mice, supporting the notion that anemia is absolutely IFNγ driven in HLH. This is consistent with other work from our lab showing that in a murine model of the related disease macrophage activation syndrome (MAS), IFNγ is absolutely required for anemia(35), work from the Jordan group using LCMV infection of *IFNγ*$^{-/-}$*Prf1*$^{-/-}$ mice showing anemia is IFNγ-dependent(36), and the IFNγ-signaling is required for anemia in IFNγR$^{-/-}$Prf1$^{-/-}$ mice too(34). No other features of HLH were reported on in *IFNγ*$^{-/-}$*Prf1*$^{-/-}$ mice by the Jordan group(36). The mechanism of how IFNγ causes anemia remains elusive. It has been established that anemia and hemophagocytes can be concurrently induced by administration of IFNγ(36), yet we show here that IFNγ is not *required* for induction of hemophagocytes, consistent with our previous report in a different model(35), and the report from the Liston group(34). This suggests that while excessive IFNγ is sufficient to induce hemophagocytosis, it is not necessary.

Why antibody-mediated blockade of IFNγ protects from HLH disease features, yet genetic absence exacerbates in some cases is an interesting conundrum. Multiple reports have shown that blockade of IFNγ in murine models of HLH is extremely effective in protecting mice from disease(3, 5). We have also repeated this in our facility and reproduce these previous findings (data not shown). Together these studies provide significant support towards investigation of IFNγ blockade as a treatment for patients with active HLH, yet it seems contradictory that patients lacking the ability to respond to IFNγ can develop disease. We show that IFNγ-blockade is not 100% efficient in preventing IFNγ signaling suggesting that low levels of IFNγ signaling constrains alternative pathological responses, and therefore absolute blockade could be detrimental to outcomes.

While we show that CD8+ T cells remain important in the manifestation of disease in LCMV-infected *IFNγ*$^{-/-}$*Prf1*$^{-/-}$ mice, specific effector cytokines that mediate the downstream immunopathology are the subject of continued investigation. Interestingly we show that an alternative cytokine signature predominates when IFNγ is absent. IL-6, IL-1β, and GM-CSF are all elevated in the absence of IFNγ, suggesting IFNγ regulation of either production, and/or accumulation of cell types that produce these cytokines. Individual blockade of these cytokines did not yield significant protection from immunopathology. It remains possible that these cytokines do not act in isolation, and that combination blockade may be effective.

Given the differences between IFNγ-sufficient and -deficient immunopathology, this model allowed the identification of some important IFNγ-driven immunoregulatory networks. The elevated GM-CSF was of particular interest to us given the extensive neutrophilia, the role of CD8+ T cells in driving disease, and that GM-CSF is made by CD8+ T cells(26, 37). Indeed, we show that *IFNγ*$^{-/-}$*Prf1*$^{-/-}$ CD8+ T cells expressed elevated levels of GM-CSF, and that exogenous administration of IFNγ regulated this production. Given the paucity of

data on GM-CSF regulation in T cells, and that T cell derived GM-CSF has an important role in other inflammatory conditions such as multiple sclerosis (MS), and the murine model of MS, experimental autoimmune encephalitis (EAE)(26, 38), there remains a need for a better understanding of this regulation. There are two major possibilities as to how IFNγ regulates the expression of GM-CSF; either GM-CSF production by CD8+ T cells is a default state in the absence of IFNγ-signaling, or that other compensatory signaling pathways that promote GM-CSF production are upregulated in the absence of IFNγ. Interestingly, there have been case reports of patients who, while on myeloablative chemotherapy, had been administered recombinant GM-CSF or the related G-CSF and developed HLH(39–41) suggesting a possible causative role for myeloid-specifying cytokines in the pathogenesis of some subsets of HLH patients.

Our study demonstrates that HLH-features can occur independent of IFNγ in a murine model, challenging the dogma that HLH pathogenesis requires IFNγ to drive disease. While IFNγ blockade may be effective in treating many cases of HLH, our study suggests that clinicians should be cognizant that HLH can occur independent of IFNγ, particularly rheumatologists that may see more of the non-classical familial forms. Differences in therapeutic response in HLH/MAS patients are likely, since HLH/MAS can be initiated by diverse triggers, on heterogenous genetic backgrounds, resulting in various downstream mediators of disease. This is in concordance with a recent study where whole-exome sequencing of HLH patients revealed a diverse set of potential disease-associated genes(42). IFNγ signatures are not always present in active HLH patients(19), and we have shown that distinct groups of patients exist that can be divided based on presence or absence of a robust IFNγ signature. Cytokines such *IL-1β* and *IL-6* remain upregulated both IFNγ-signature high, and low patient groups, and in the IFNγ-independent murine model of HLH presented in this report. It is intriguing to note that while not effective in the murine system presented here, IL-1β blockade has been reported to be effective in other human forms of HLH/MAS(43). Clearly, the central cytokines controlling MAS/HLH vary in different scenarios, with continued work needed to dissect all of these nuances.

Even in the absence of IFNγ, we show that CD8+ T cells remain critically important for disease. This suggests that modulators of CD8+ T cell activation such as IL-33:ST2(21), rather than blockade of downstream effector molecules, may be a more universally effective way to treat HLH. The effectiveness of this blockade in other models(7), including the *IFNγ*$^{-/-}$*Prf1*$^{-/-}$ model used in this study, suggests this may be an effective treatment for HLH patients, and warrants further investigation. Taken together, this report demonstrates that HLH can occur independently of IFNγ, offering insights into potential alternative disease mechanisms and alternative treatment strategies that may be effective in clinical scenarios when IFNγ blockade is insufficient to ameliorate clinical manifestations of life-threatening HLH.

Supplementary Material

Refer to Web version on PubMed Central for supplementary material.

ACKNOWLEDGMENTS

The authors thank Dirk Smith for providing α-ST2 and control antibodies.

This study was supported by National Institutes of Health National Heart, Lung, and Blood Institute grant RO1 HL112836-A1 (E.M.B.); National Institute of Allergy and Infectious Diseases RO1 AI121250-A1 (E.M.B.); and the Nancy Taylor Foundation for Chronic Disease (E.M.B.).

Supporting Grants:

This study was supported by National Institutes of Health National Heart, Lung, and Blood Institute grant R01 HL112836-A1 (E.M.B.); National Institute of Allergy and Infectious Diseases R01 AI121250-A1 (E.M.B.); and the Nancy Taylor Foundation for Chronic Disease (E.M.B.).

REFERENCES

1. Brisse E, Wouters C,H, Matthys P Hemophagocytic lymphohistiocytosis (HLH): A heterogeneous spectrum of cytokine-driven immune disorders. Cytokine & Growth Factor Reviews. 2015;26(3): 263280. doi: 10.1016/j.cytogfr.2014.10.001.
2. Stepp SE, Dufourcq-Lagelouse R, Le Deist F, Bhawan S, Certain S, Mathew PA, et al. Perforin gene defects in familial hemophagocytic lymphohistiocytosis. Science (New York, NY). 1999;286(5446): 1957–9. doi: 10.1126/science.286.5446.1957.
3. Jordan MB, Hildeman D, Kappler J, Marrack P. An animal model of hemophagocytic lymphohistiocytosis (HLH): CD8+ T cells and interferon gamma are essential for the disorder. Blood. 2004;104(3):735–43. doi: 10.1182/blood-2003-10-3413. [PubMed: 15069016]
4. Jenkins MR, Rudd-Schmidt JA, Lopez JA, Ramsbottom KM, Mannering SI, Andrews DM, et al. Failed CTL/NK cell killing and cytokine hypersecretion are directly linked through prolonged synapse time. The Journal of Experimental Medicine. 2015;212(3):307–17. doi: 10.1084/jem.20140964. [PubMed: 25732304]
5. Pachlopnik Schmid J, Ho CH, Chrétien F, Lefebvre JM, Pivert G, Kosco-Vilbois M, et al. Neutralization of IFNγ defeats haemophagocytosis in LCMV-infected perforin- and Rab27a-deficient mice. EMBO Molecular Medicine. 2009;1(2):112–24. doi: 10.1002/emmm.200900009. [PubMed: 20049711]
6. Rood JE, Rao S, Paessler M, Kreiger PA, Chu N, Stelekati E, et al. ST2 contributes to T-cell hyperactivation and fatal hemophagocytic lymphohistiocytosis in mice. Blood. 2016;127(4):426–35. Epub 2015/11/01. doi: 10.1182/blood-2015-07-659813. [PubMed: 26518437]
7. Taylor MD, Burn TN, Wherry EJ, Behrens EM. CD8 T Cell Memory Increases Immunopathology in the Perforin-Deficient Model of Hemophagocytic Lymphohistiocytosis Secondary to TNF-α. 2018. doi: 10.4049/immunohorizons.1800003.
8. Jordan M, Locatelli F, Allen C, De Benedetti F, Grom AA, Ballabio M, et al. A Novel Targeted Approach to the Treatment of Hemophagocytic Lymphohistiocytosis (HLH) with an Anti-Interferon Gamma (IFNγ) Monoclonal Antibody (mAb), NI-0501: First Results from a Pilot Phase 2 Study in Children with Primary HLH. 2015.
9. Henter JI, Horne A, Arico M, Egeler RM, Filipovich AH, Imashuku S, et al. HLH-2004: Diagnostic and therapeutic guidelines for hemophagocytic lymphohistiocytosis. Pediatr Blood Cancer. 2007;48(2):124–31. Epub 2006/08/29. doi: 10.1002/pbc.21039. [PubMed: 16937360]
10. Brisse E, Imbrechts M, Mitera T, Vandenhaute J, Berghmans N, Boon L, et al. Lymphocyte-independent pathways underlie the pathogenesis of murine cytomegalovirus-associated secondary haemophagocytic lymphohistiocytosis. Clinical & Experimental Immunology. 2018;192(1):104–19. Epub 2017/11/28. doi: 10.1111/cei.13084. [PubMed: 29178470]
11. van Dommelen S, Sumaria N, Schreiber RD, Scalzo AA, Smyth MJ, Degli-Esposti MA. Perforin and Granzymes Have Distinct Roles in Defensive Immunity and Immunopathology. Immunity. 2006;25(5):835–48. doi: 10.1016/j.immuni.2006.09.010. [PubMed: 17088087]
12. Tesi B, Sieni E, Neves C, Romano F, Cetica V, Cordeiro AI, et al. Hemophagocytic lymphohistiocytosis in 2 patients with underlying IFN-γ receptor deficiency. The Journal of

allergy and clinical immunology. 2015;135(6):1638–41. doi: 10.1016/j.jaci.2014.11.030. [PubMed: 25592983]

13. Staines-Boone AT, Deswarte C, Venegas Montoya E, Sanchez-Sanchez LM, Garcia Campos JA, Muniz-Ronquillo T, et al. Multifocal Recurrent Osteomyelitis and Hemophagocytic Lymphohistiocytosis in a Boy with Partial Dominant IFN-gammaR1 Deficiency: Case Report and Review of the Literature. Front Pediatr. 2017;5:75 Epub 2017/05/19. doi: 10.3389/fped.2017.00075. [PubMed: 28516082]
14. Burns C, Cheung A, Stark Z, Choo S, Downie L, White S, et al. A novel presentation of homozygous loss-of-function STAT-1 mutation in an infant with hyperinflammation-A case report and review of the literature. J Allergy Clin Immunol Pract. 2016;4(4):777–9. Epub 2016/04/28. doi: 10.1016/j.jaip.2016.02.015. [PubMed: 27117246]
15. Krebs P, Crozat K, Popkin D, Oldstone M, B., Beutler B. Disruption of MyD88 signaling suppresses hemophagocytic lymphohistiocytosis in mice. Blood. 2011;117(24):6582–8. doi: 10.1182/blood-2011-01-329607. [PubMed: 21551232]
16. Nansen A, Jensen T, Christensen JP, Andreasen SØ, Röpke C, Marker O, et al. Compromised Virus Control and Augmented Perforin-Mediated Immunopathology in IFN-γ-Deficient Mice Infected with Lymphocytic Choriomeningitis Virus. Journal of Immunology. 1999.
17. Avau A, Mitera T, Put S, Put K, Brisse E, Filtjens J, et al. Systemic juvenile idiopathic arthritis-like syndrome in mice following stimulation of the immune system with Freund's complete adjuvant: regulation by interferon-γ. Arthritis & Rheumatology. 2014;66(5):1340–51. doi: 10.1002/art.38359. [PubMed: 24470407]
18. Ahmed R, Salmi A, Butler LD, Chiller JM, Oldstone MB. Selection of genetic variants of lymphocytic choriomeningitis virus in spleens of persistently infected mice. Role in suppression of cytotoxic T lymphocyte response and viral persistance. J Exp Med. 1984;160(2):521–40. [PubMed: 6332167]
19. Sumegi J, Barnes MG, Nestheide SV, Molleran-Lee S, Villanueva J, Zhang K, et al. Gene expression profiling of peripheral blood mononuclear cells from children with active hemophagocytic lymphohistiocytosis. Blood. 2011;117(15):60. doi: 10.1182/blood-2010-08-300046.
20. Palmer G, Talabot-Ayer D, Lamacchia C, Toy D, Seemayer CA, Viatte S, et al. Inhibition of interleukin-33 signaling attenuates the severity of experimental arthritis. Arthritis & Rheumatology. 2009;60(3):738–49. Epub 2009/02/28. doi: 10.1002/art.24305.
21. Rood JE, Rao S, Paessler M, Kreiger PA, Chu N, Stelekati E, et al. ST2 contributes to T-cell hyperactivation and fatal hemophagocytic lymphohistiocytosis in mice. Blood. 2016;127(4):426–35. doi: 10.1182/blood-2015-07-659813. [PubMed: 26518437]
22. Badovinac VP, Tvinnereim AR, Harty JT. Regulation of Antigen-Specific CD8+ T Cell Homeostasis by Perforin and Interferon-γ. 2000. doi: 10.1126/science.290.5495.1354.
23. Copenhaver AM, Casson CN, Nguyen HT, Duda MM, Shin S. IL-1R signaling enables bystander cells to overcome bacterial blockade of host protein synthesis. Proc Natl Acad Sci U S A. 2015;112(24):7557–62. doi: 10.1073/pnas.1501289112. [PubMed: 26034289]
24. Barber DL, Andrade BB, McBerry C, Sereti I, Sher A. Role of IL-6 in Mycobacterium avium--associated immune reconstitution inflammatory syndrome. Journal of Immunology. 2014;192(2):676–82. Epub 2013/12/18. doi: 10.4049/jimmunol.1301004.
25. Samavedam UK, Iwata H, Muller S, Schulze FS, Recke A, Schmidt E, et al. GM-CSF modulates autoantibody production and skin blistering in experimental epidermolysis bullosa acquisita. Journal of Immunology. 2014;192(2):559–71. Epub 2013/12/18. doi: 10.4049/jimmunol.1301556.
26. Rasouli J, Ciric B, Imitola J, Gonnella P, Hwang D, Mahajan K, et al. Expression of GM-CSF in T Cells Is Increased in Multiple Sclerosis and Suppressed by IFN-β Therapy. Journal of Immunology. 2015;194(11). doi: 10.4049/jimmunol.1403243.
27. Al-Mossawi M, Chen L, Fang H, Ridley A, Wit J, Yager N, et al. Unique transcriptome signatures and GM-CSF expression in lymphocytes from patients with spondyloarthritis. Nature Communications. 2017;8(1):1510. doi: doi:10.1038/s41467-017-01771-2.
28. Lehmberg K, Pink I, Eulenburg C, Beutel K, Maul-Pavicic A, Janka G. Differentiating macrophage activation syndrome in systemic juvenile idiopathic arthritis from other forms of hemophagocytic

lymphohistiocytosis. The Journal of Pediatrics. 2013;162(6):1245–51. Epub 2013/01/22. doi: 10.1016/j.jpeds.2012.11.081. [PubMed: 23333131]

29. Pillay J, den Braber I, Vrisekoop N, Kwast L, de Boer R, Borghans J, et al. In vivo labeling with 2H2O reveals a human neutrophil lifespan of 5.4 days. Blood. 2010. doi: 10.1182/blood-2010-01-259028.
30. Yazdani HO, Chen HW, Tohme S, Tai S, van der Windt DJ, Loughran P, et al. IL-33 exacerbates liver sterile inflammation by amplifying neutrophil extracellular trap formation. J Hepatol. 2017 Epub 2017/09/26. doi: 10.1016/j.jhep.2017.09.010.
31. Bartholdy C, Høgh-Petersen M, Storm P, Holst P, Ørskov C, Christensen J, et al. IFNγ and Perforin Cooperate to Control Infection and Prevent Fatal Pathology During Persistent Gammaherpesvirus Infection in Mice. Scandinavian Journal of Immunology. 2014;79(6):395–403. doi: 10.1111/sji.12176. [PubMed: 24684620]
32. Brisse E, Imbrechts M, Put K, Avau A, Mitera T, Berghmans N, et al. Mouse Cytomegalovirus Infection in BALB/c Mice Resembles Virus-Associated Secondary Hemophagocytic Lymphohistiocytosis and Shows a Pathogenesis Distinct from Primary Hemophagocytic Lymphohistiocytosis. J Immunol. 2016;196(7):3124–34. Epub 2016/02/24. doi: 10.4049/jimmunol.1501035. [PubMed: 26903481]
33. Put K, Brisse E, Avau A, Imbrechts M, Mitera T, Janssens R, et al. IDO1 Deficiency Does Not Affect Disease in Mouse Models of Systemic Juvenile Idiopathic Arthritis and Secondary Hemophagocytic Lymphohistiocytosis. PLoS One. 2016;11(2):e0150075 Epub 2016/02/26. doi: 10.1371/journal.pone.0150075. [PubMed: 26914138]
34. Humblet-Baron S ea. IFN-γ and CD25 drive distinct pathologic features during hemophagocytic lymphohistiocytosis. J Allergy Clin Immunol. 2019;143(6):2215–26. [PubMed: 30578871]
35. Canna SW, Wrobel J, Chu N, Kreiger PA, Paessler M, Behrens EM. Interferon-γ mediates anemia but is dispensable for Fulminant Toll-Like Receptor 9-induced Macrophage Activation Syndrome and Hemophagocytosis. Arthritis & Rheumatology. 2013;65(7):1764–75. doi: 10.1002/art.37958.
36. Zoller E, Lykens J, Terrell C, Aliberti J, Filipovich A, Henson P, et al. Hemophagocytosis causes a consumptive anemia of inflammation. The Journal of Experimental Medicine. 2011;208(6):1203–14. doi: 10.1084/jem.20102538. [PubMed: 21624938]
37. Rothchild AC, Stowell B, Goyal G, Nunes-Alves C, Yang Q, Papavinasasundaram K, et al. Role of Granulocyte-Macrophage Colony-Stimulating Factor Production by T Cells during Mycobacterium tuberculosis Infection. mBio. 2017;8(5). doi: 10.1128/mBio.01514-17.
38. Croxford A, Lanzinger M, Hartmann F, Schreiner B, Mair F, Pelczar P, et al. The Cytokine GM-CSF Drives the Inflammatory Signature of CCR2+ Monocytes and Licenses Autoimmunity. Immunity. 2015;43(3):502–14. doi: 10.1016/j.immuni.2015.08.010. [PubMed: 26341401]
39. Wang S, Degar BA, Zieske A, Shafi NQ, Rose MG. Hemophagocytosis exacerbated by G-CSF/GM-CSF treatment in a patient with myelodysplasia. American Journal of Hematology. 2004;77(4):391–6. doi: 10.1002/ajh.20202. [PubMed: 15551287]
40. Glasser L, LeGolvan M, Horwitz H, M. Florid histiocytic hemophagocytosis following therapy with long acting G-CSF (pegfilgrastim). American Journal of Hematology. 2007;82(8):753–7. doi: 10.1002/ajh.20854. [PubMed: 17315211]
41. Padhi S, Varghese RG, Ramdas A, Phansalkar MD, Sarangi R. Hemophagocytic lymphohistiocytosis: critical reappraisal of a potentially under-recognized condition. - PubMed - NCBI Frontiers of Medicine 2013;7(4):492–98. [PubMed: 24127015]
42. Chinn I, Eckstein O, Peckham-Gregory E, Goldberg B, Forbes L, Nicholas S, et al. Genetic and mechanistic diversity in pediatric hemophagocytic lymphohistiocytosis. Blood. 2018;132(1):89–100. doi: 10.1182/blood-2017-11-814244. [PubMed: 29632024]
43. Miettunen PM, Narendran A, Jayanthan A, Behrens EM, Cron RQ. Successful treatment of severe paediatric rheumatic disease-associated macrophage activation syndrome with interleukin-1 inhibition following conventional immunosuppressive therapy: case series with 12 patients. Rheumatology. 2011;50(2):417–9. doi: 10.1093/rheumatology/keq218. [PubMed: 20693540]

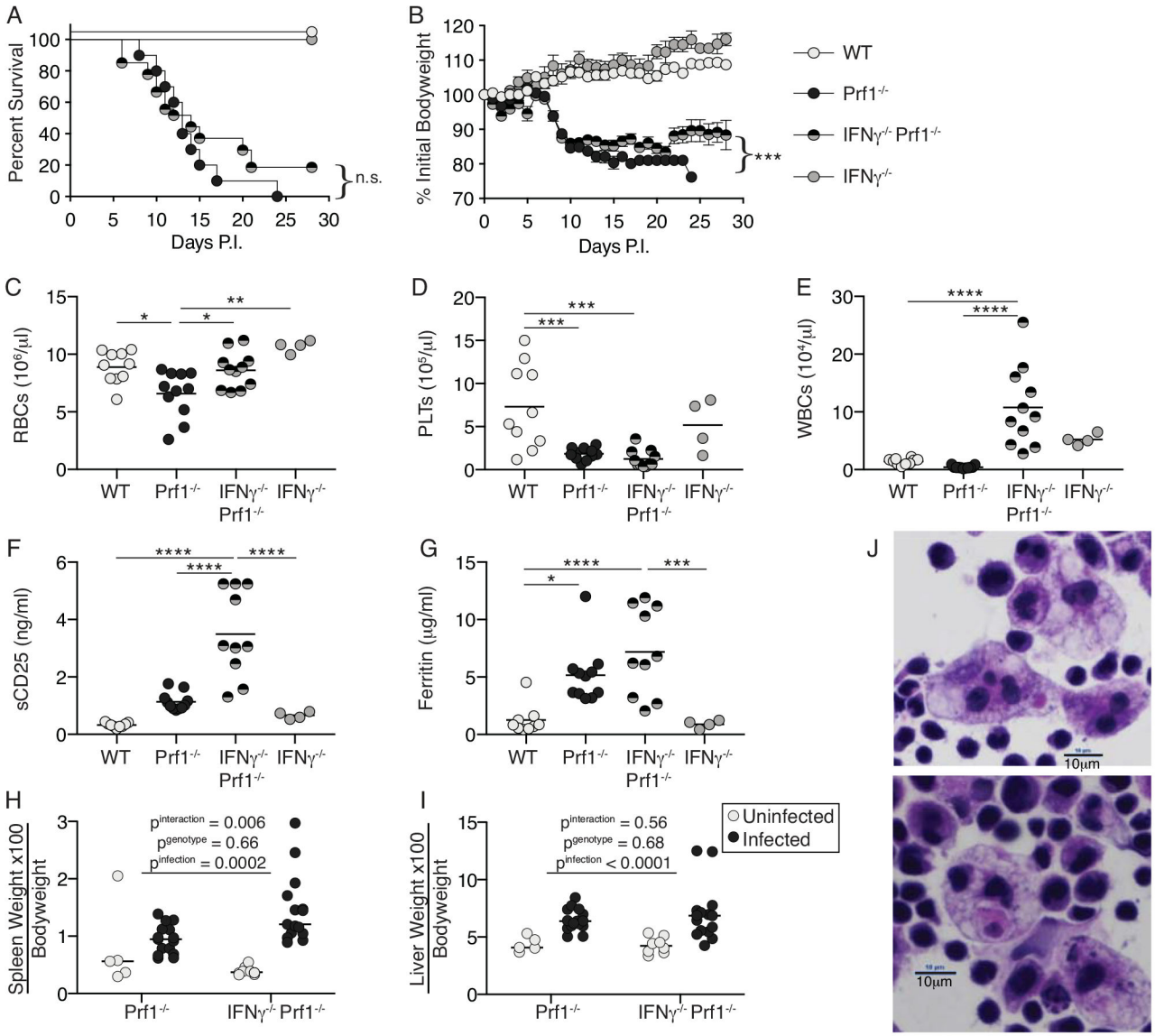

Figure 1: IFNγ$^{-/-}$Prf1$^{-/-}$ mice succumb to HLH-like disease

WT(n=8), *Prf1*$^{-/-}$(n=10), *IFNγ*$^{-/-}$*Prf1*$^{-/-}$(n=27), or *IFNγ*$^{-/-}$(n=5) mice were infected with LCMV-Armstrong and survival (A), and weight-loss (B) were monitored. Data combined from 2-independent experiments. Survival curves (A) analyzed by log-rank (Mantel-Cox) test. Weight-loss (B) analyzed by linear mixed-effects model to allow for missing data due to mouse mortality: treatment and body weight were modeled as fixed effects, and individual mice were treated as a random effect to account for baseline variability between animals (e.g. intercept only). Symbols indicate mean and SEM. Mice were infected with LCMV and then sacrificed day-10 post-infection. Complete blood counts were performed and red blood cells (C), platelets (D), and white blood cells (E) were enumerated. Serum levels of soluble CD25 (F) and ferritin (G) were measured by ELISA from Day-10 infected mice. Data combined from N=2 individual experiments. Analyzed by 1-way ANOVA with Tukey HSD post-test. n.s. p>0.05, *p<0.05, **p<0.01, ***p<0.001, ****p<0.0001. (H) Spleen and (I) Livers were from day 10 infected, or uninfected controls were weighed and normalized to

bodyweight pre-infection. Analyzed by 2-way ANOVA. (J) H&E stained splenic touch-preps from day 10 infected *IFNγ*$^{-/-}$*Prf1*$^{-/-}$ mice showing presence of hemophagocytes. Total magnification = 600x.

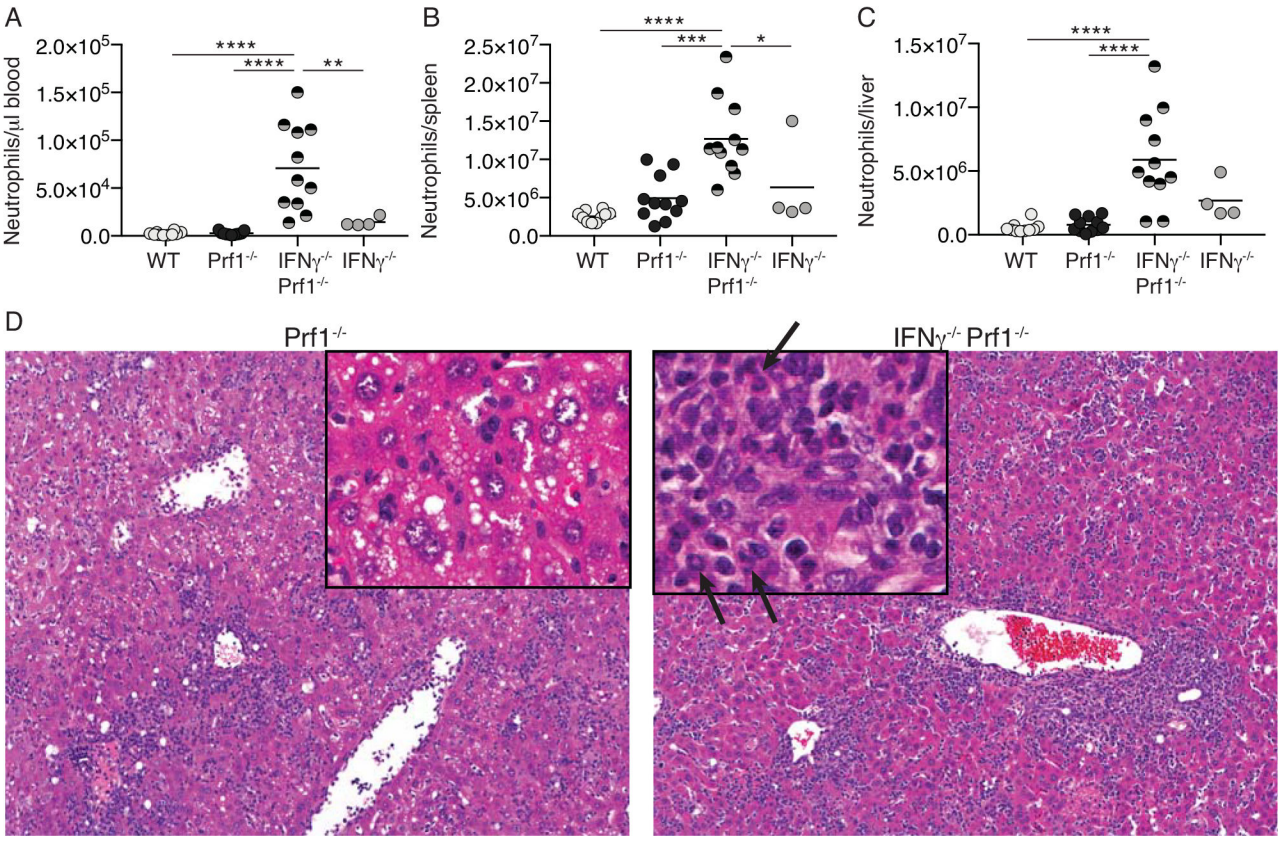

Figure 2: IFNγ$^{-/-}$Prf1$^{-/-}$ mice display extensive neutrophilia

WT, *Prf1*$^{-/-}$, *IFNγ*$^{-/-}$*Prf1*$^{-/-}$, and *IFNγ*$^{-/-}$ mice were infected with LCMV and neutrophils were quantified in the blood (A), spleen (B), and liver (C) day-10 post-infection by flow cytometry. Neutrophils were designated as live, singlets, CD90.2-, CD19-, CD11b+, Ly6G+ (Gating=Supplemental Figure 3). Data combined from N=2 individual experiments. Analyzed by 1-way ANOVA with Tukey HSD post-test. *p<0.05, **p<0.01, ***p<0.001, ****p<0.0001. (D) Representative H&E-stained liver sections from *Prf1*$^{-/-}$ (left) and *IFNγ*$^{-/-}$*Prf1*$^{-/-}$ (right) mice on day 10 post-infection. Original magnification=100X, inset=200X. Arrows indicate ringed/multi-lobed nuclei typical of murine neutrophils.

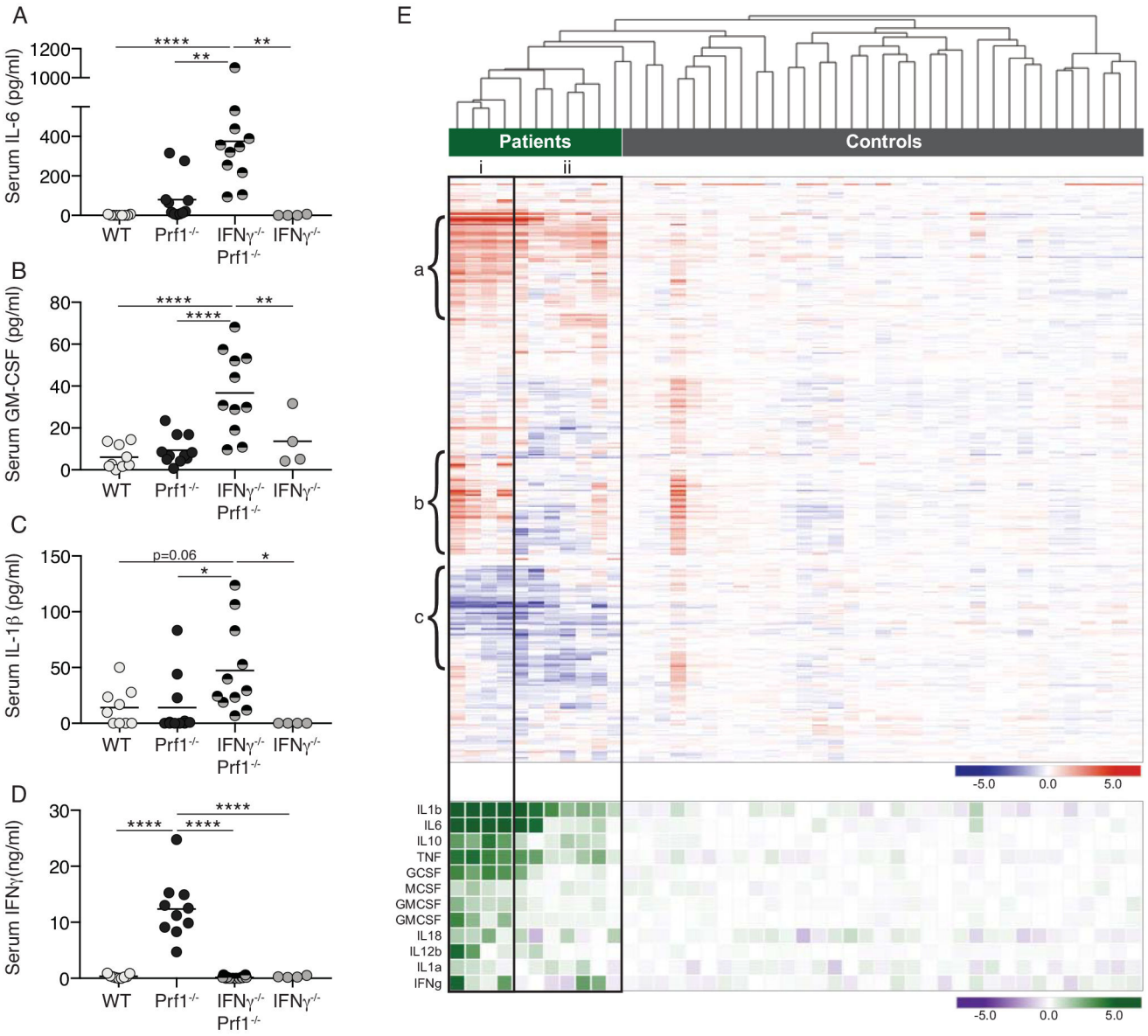

Figure 3: Altered cytokine milieu in *IFNγ*$^{-/-}$*Prf1*$^{-/-}$ mice corresponds with cytokine expression in human HLH patients

WT, *Prf1*$^{-/-}$, *IFNγ*$^{-/-}$*Prf1*$^{-/-}$, and *IFNγ*$^{-/-}$ mice were infected with LCMV and serum was obtained day-10 post-infection. IL-6 (A), GM-CSF (B), IL-1β (C), and IFNγ (D) was measured by ELISA. Data combined from N=2 individual experiments. Analyzed by 1-way ANOVA with Tukey HSD post-test. *p<0.05, **p<0.01, ***p<0.001, ****p<0.0001. (E-TOP) Gene expression dataset from HLH patients and controls (GSE26050, (19)) was filtered on the curated IFNγ-gene set (MSigDB, Broad) and subjected to unsupervised hierarchical clustering. (E-BOTTOM) Expression of additional selected cytokines shown according to clustering based on IFNγ-gene set. Columns indicate individual patients.

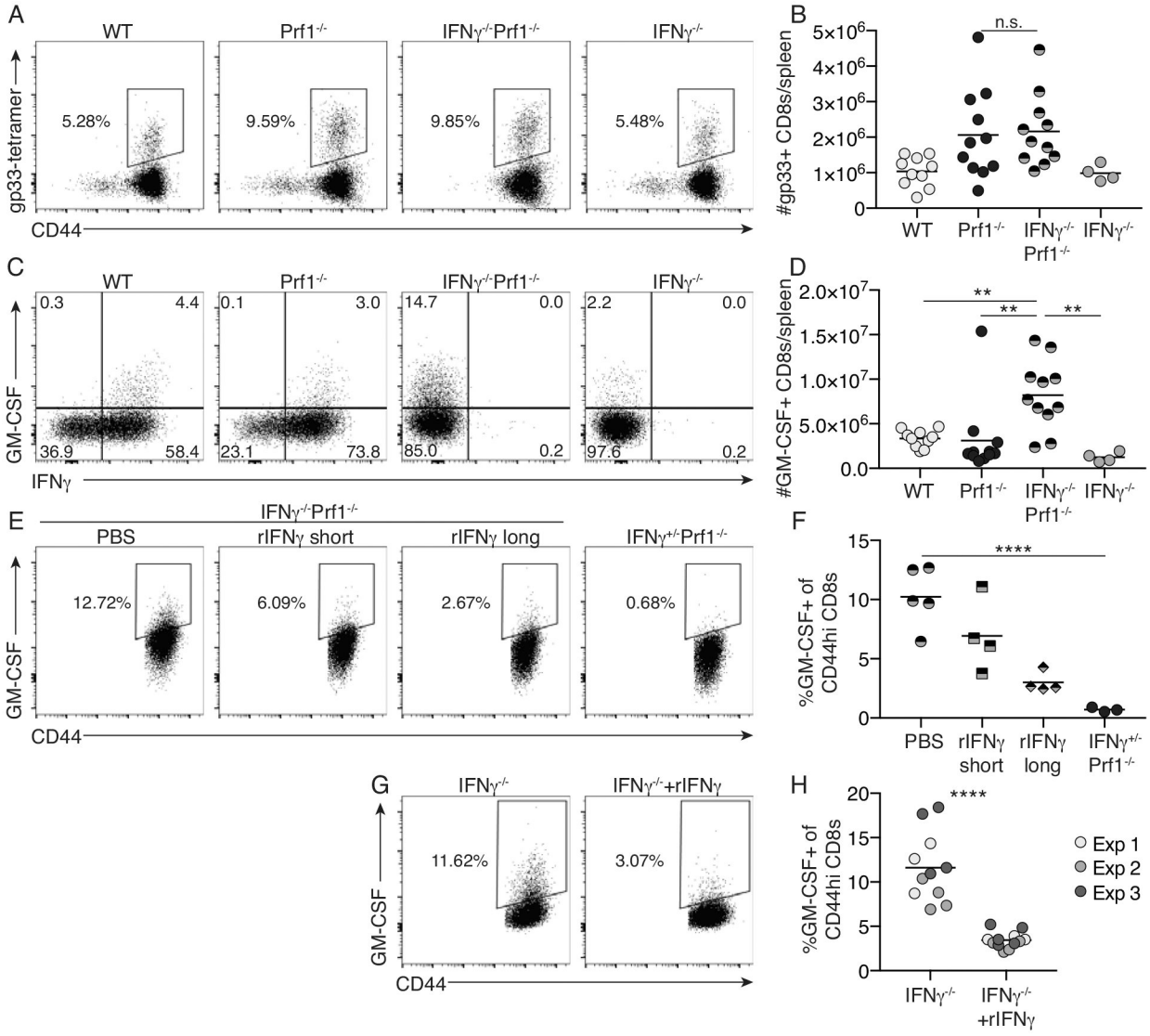

Figure 4: CD8+ T cells from *IFNγ*$^{-/-}$*Prf1*$^{-/-}$ mice have elevated expression of GM-CSF that is regulated by IFNγ

WT, *Prf1*$^{-/-}$, *IFNγ*$^{-/-}$*Prf1*$^{-/-}$, and *IFNγ*$^{-/-}$ mice were infected with LCMV and sacrificed day 10 post-infection. LCMV-specific CD8+ T cells were identified by H-2K^{b}-gp33 tetramer staining. (A) Representative flow plots gated on live, singlets, CD90.2+, CD8+ cells. (B) Total number of H-2K^{b}-gp33+ CD44+ CD8+ T cells in spleens of day 10 infected mice. Data combined from N=2 independent experiments. Analyzed by 1-way ANOVA with Tukey HSD post-test. (C) Splenocytes from day 10 infected mice were stimulated by PMA & ionomycin and IFNγ/GM-CSF expression was analyzed as described in methods. Representative flow plots of live, singlet, CD90.2+, CD8+, CD44hi cells (Supplemental Figure 4). (D) Total GM-CSF+ CD44hi CD8+ T cells per spleen of day 10 infected mice. Data combined from N=2 independent experiments. Analyzed by 1-way ANOVA with Tukey HSD post-test. (E) *IFNγ*$^{-/-}$*Prf1*$^{-/-}$ or *IFNγ*$^{+/-}$*Prf1*$^{-/-}$ littermate controls were infected with LCMV. *IFNγ*$^{-/-}$*Prf1*$^{-/-}$ mice were administered either PBS, recombinant IFNγ (rIFNγ) beginning day 0 (rIFNγ long), or rIFNγ from day 6 (rIFNγ short), by

intraperitoneal injection every other day. Mice were sacrificed day 10 post-infection and GM-CSF expression was analyzed as in (C). (E) Representative flow plots of live, singlets, CD90.2+, CD8+, CD44hi cells. (F) Summary data showing frequency of GM-CSF expressing CD44hi CD8+ T cells from IFNγ-giveback experiment. Analyzed by ANOVA with test for linear trend. (G) Naïve CD8+ T cells from uninfected *IFNγ*$^{-/-}$ mice (purity <90%) were cultured *in vitro* in the presence or absence of rIFNγ for 5 days and then analyzed for GM-CSF expression as described in methods. (G) Representative flow plots of live, singlets, CD90.2+, CD8+, CD44hi cells. (H) Summary data showing frequency of GM-CSF+, CD44hi, CD8+ T cells. Data combined from N=3 independent experiments. Analyzed by 2-tailed, unpaired student's t-test. n.s. $p>0.05$, **$p<0.01$, ***$p<0.001$, ****$p<0.0001$

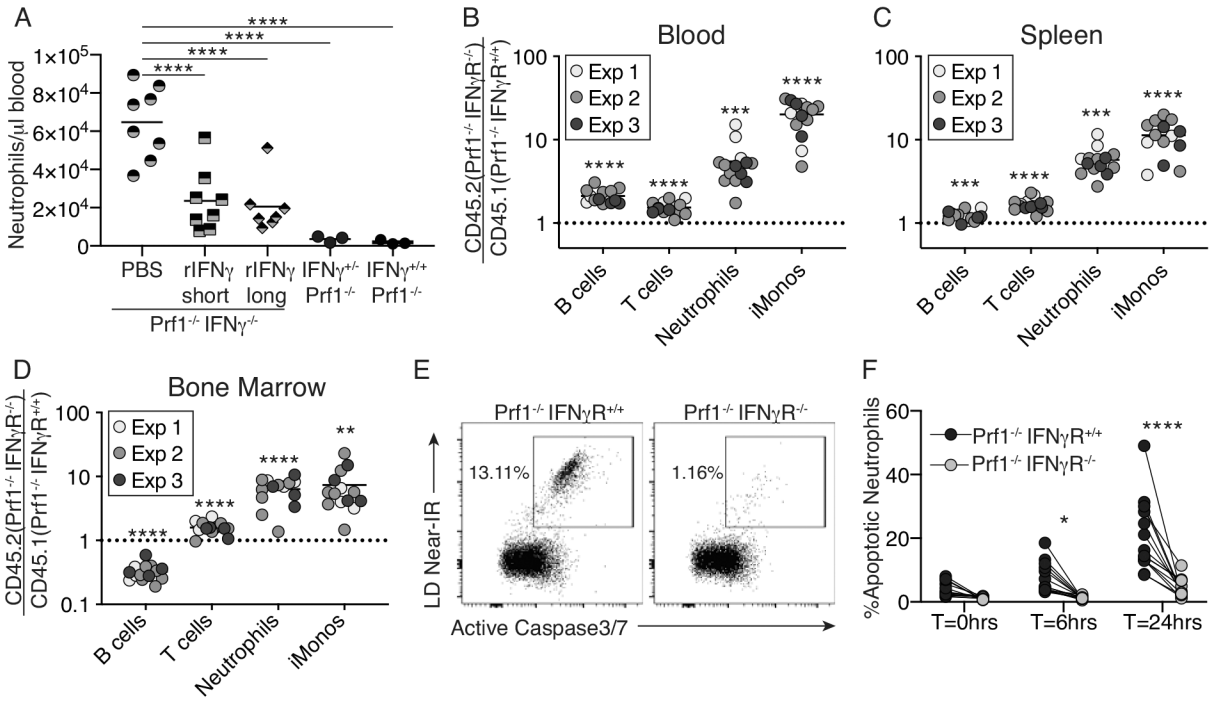

Figure 5: Neutrophil-intrinsic IFNγ-signaling regulates neutrophilia through enhanced cell death

(A) *IFNγ*$^{-/-}$*Prf1*$^{-/-}$, *IFNγ*$^{+/+}$*Prf1*$^{-/-}$, or *IFNγ*$^{+/-}$*Prf1*$^{-/-}$ littermate controls were infected with LCMV. *IFNγ*$^{-/-}$*Prf1*$^{-/-}$ mice were intraperitoneally administered PBS, recombinant IFNγ (rIFNγ) beginning day 0 (rIFN-long), or rIFNγ from day 6 (rIFNγ-short) every other day. Mice were sacrificed day 10 post-infection and blood neutrophils were quantified by flow cytometry. Data combined from N=2 independent experiments. Analyzed by 1-way ANOVA with Tukey HSD post-test. Bone chimeras reconstituted from 50:50 *Prf1*$^{-/-}$*IFNγR*$^{+/+}$: *Prf1*$^{-/-}$*IFNγR*$^{-/-}$ mix of donor bone marrow were generated. Chimeras were infected with LCMV and sacrificed 10 days post-infection. (B-D) The ratio of specific cell-types derived from *Prf1*$^{-/-}$*IFNγR*$^{-/-}$*CD45.2*$^{+}$ vs. *Prf1*$^{-/-}$*IFNγR*$^{+/+}$*CD45.1*$^{+}$ donor bone marrow was determined and normalized to pre-infection ratios in the blood. Data combined from N=3 independent experiments. Analyzed by 1-sample Student's *t*-test for each cell type against the null-ratio=1. (E-F) Bone marrow from chimeras on day 10 post-infection was cultured *ex vivo* and measured for cell permeability and Active Caspase-3/7 in neutrophils cultured for indicated time. (E) representative flow plots of neutrophils from *Prf1*$^{-/-}$*IFNγR*$^{+/+}$ (left) or *Prf1*$^{-/-}$*IFNγR*$^{-/-}$ (right) donors from the same chimeric mouse, cultured for 24hours. (F) Summary data showing %apoptotic neutrophils at multiple time-points. Lines connect cells from same chimeric mouse. Analyzed by 2-way repeated measures ANOVA with Sidak multiple comparison post-test. *p<0.05,**p<0.01,***p<0.001,****p<0.0001

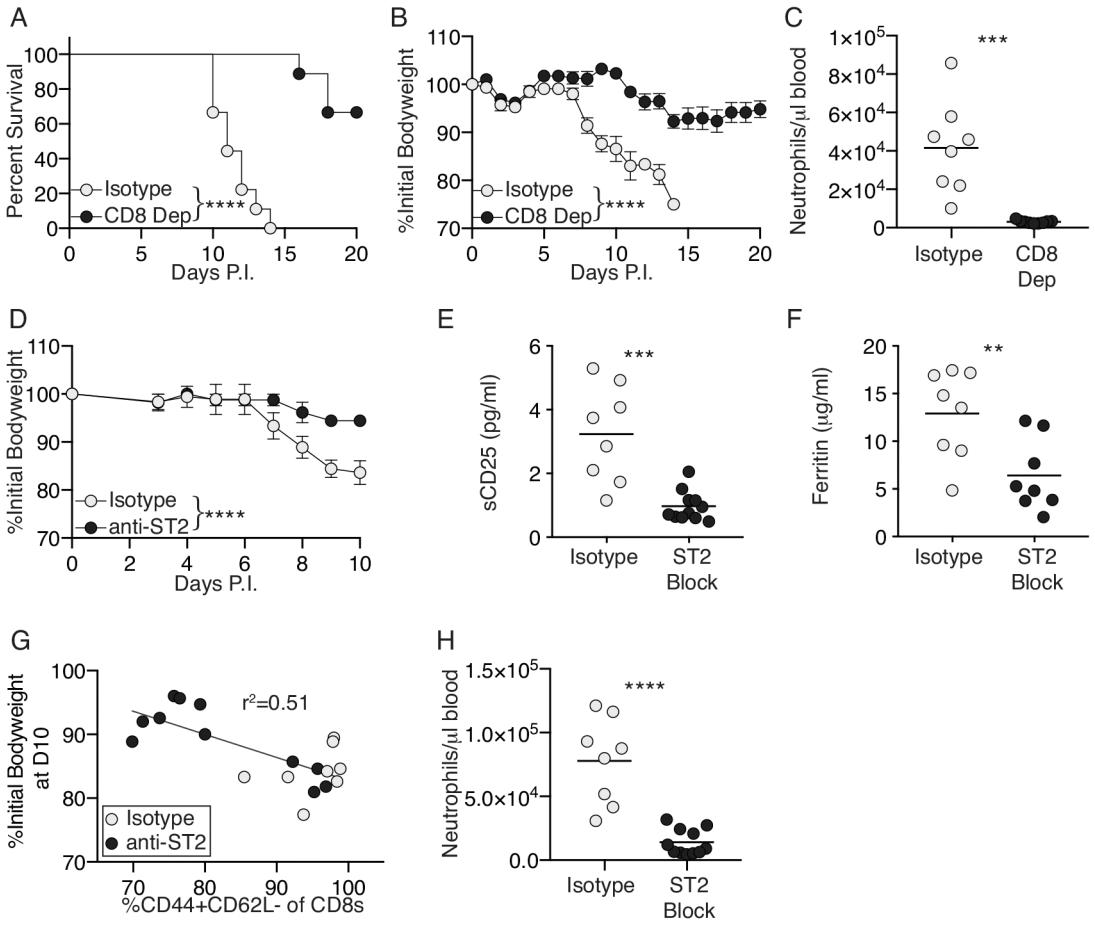

Figure 6: CD8+ T cells and IL-33-signaling remain pathological drivers of disease in the absence of IFNγ

(A,B) *IFNγ*$^{-/-}$*Prf1*$^{-/-}$ mice were infected with LCMV and administered CD8-depleting antibody, or isotype control, beginning day 3 post-infection and every other day thereafter, n=9 mice per group. Survival (A), and weight loss (B) were measured. Survival curve (A) analyzed by log-rank (Mantel-Cox) test. Weight-loss (B) analyzed by linear mixed-effects model as in Figure 1. Symbols indicate mean±SEM. (C) *IFNγ*$^{-/-}$*Prf1*$^{-/-}$ mice were infected and treated with CD8-depleting or isotype control antibody. Neutrophils were quantified in the blood on day 10 post infection. Data combined from N=2 independent experiments. Analyzed by 2-way unpaired Student's *t*-test. (D-H) *IFNγ*$^{-/-}$*Prf1*$^{-/-}$ mice were infected with LCMV and administered ST2 blocking antibody (anti-ST2), or isotype control beginning day 3 post-infection and every other day thereafter. (D) Weight loss was measured and analyzed as before. n=4 mice per group, representative data from 1 of 3 independent experiments. (E) Serum sCD25 and (F) serum ferritin, from Day 10 infected mice, data combined from N=3 independent experiments. Analyzed by 2-way unpaired Student's *t*-test. (G) Frequency of CD44+CD62L- of CD8+ T cells (live,singlets,CD90.2+,CD8+; Supplemental Figure-8) was plotted against total weight loss observed by day 10 post-infection. Data combined from N=3 individual experiments. Analyzed by linear regression using single curve for all data sets. (F) Neutrophils were quantified in the blood on day 10 post infection from anti-ST2 or isotype treated *IFNγ*$^{-/-}$*Prf1*$^{-/-}$ mice. Data combined from

N=3 independent experiments. Analyzed by 2-way unpaired Student's *t*-test.
p<0.01,*p<0.001,****p<0.0001